

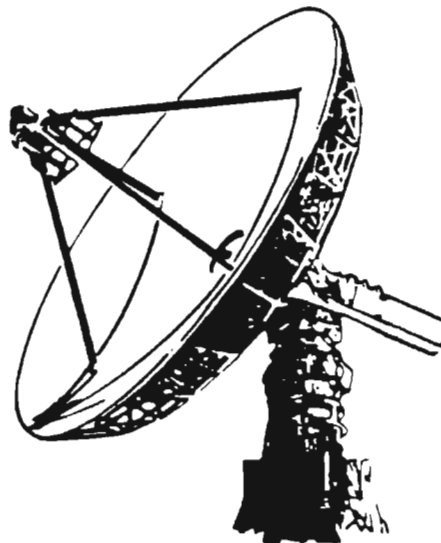
# AN ANALYSIS OF VECTOR MEASUREMENT ACCURACY ENHANCEMENT TECHNIQUES

DOUG RYTTING  
NETWORK MEASUREMENTS DIVISION  
1400 FOUNTAIN GROVE PARKWAY  
SANTA ROSA, CALIFORNIA 95401

**RF & Microwave  
Measurement  
Symposium  
and  
Exhibition**



**HEWLETT  
PACKARD**



# AN ANALYSIS OF VECTOR MEASUREMENT ACCURACY ENHANCEMENT TECHNIQUES

Vector measurements require both magnitude and phase data. Some typical examples are the complex reflection coefficient, the magnitude and phase of the transfer function, and the group delay.

## AGENDA

- ACCURACY ENHANCEMENT FOR ONE-PORT NETWORKS
- ONE-PORT CALIBRATION TECHNIQUES
- ACCURACY ENHANCEMENT FOR TWO-PORT NETWORKS
- TWO-PORT CALIBRATION TECHNIQUES

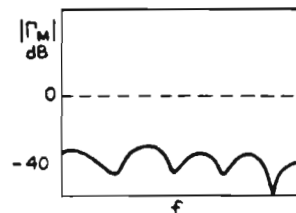
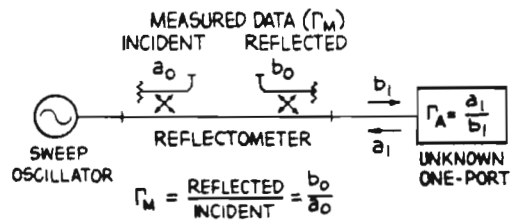
The seminar will cover four basic topics: (1) A review of accuracy enhancement for one-port networks. (2) One-port calibration techniques. (3) Accuracy enhancement for two-port networks, and (4) two-port calibration techniques.

This section reviews the basic theory of accuracy enhancement for one-port networks.

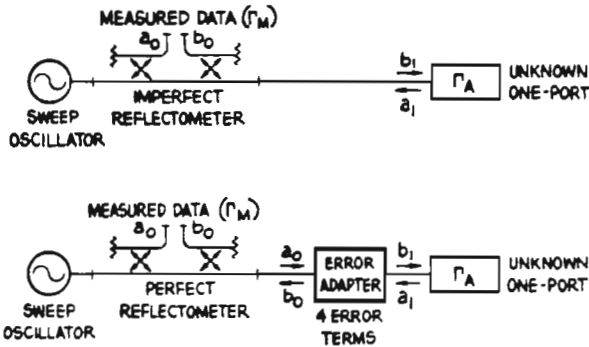
# ACCURACY ENHANCEMENT FOR ONE-PORT NETWORKS

The block diagram of the measurement system consists of a sweep oscillator, a reflectometer consisting of two couplers connected back-to-back, and the unknown one-port ( $\Gamma_A$ ). The direction of power flow through the system is indicated by the arrows. The measured reflection coefficient is defined as  $\Gamma_M$ . The measurement system is not perfect and contributes errors to the measurement of  $\Gamma_A$ . For example, a one-port network (an ideal resistive termination which has a 40 dB return loss), has a well behaved frequency response. But the measured  $\Gamma_M$  still typically has 10 dB peak-to-peak variations with respect to frequency. The variations are not in the resistive device. An ideal resistor is incapable of causing this type of changing reflection coefficient. The errors in this case are in the measurement system.

## THE PROBLEM ONE-PORT



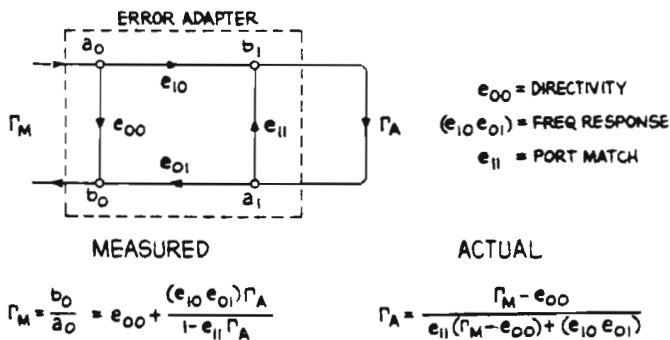
# ONE-PORT ERROR MODELING



The following is a discussion of the various errors that are inherent in a reflectometer.

An imperfect reflectometer can be modeled by taking all the linear errors of the system and combining them into a fictitious two-port error adapter between the reflectometer and the unknown one-port. This results in an absolutely perfect reflectometer with no loss, no mismatch, and no frequency response errors. The fictitious two-port error adapter has four error terms. When making ratio measurements, only three terms are needed.

# ONE-PORT FLOW GRAPH AND SOLUTION

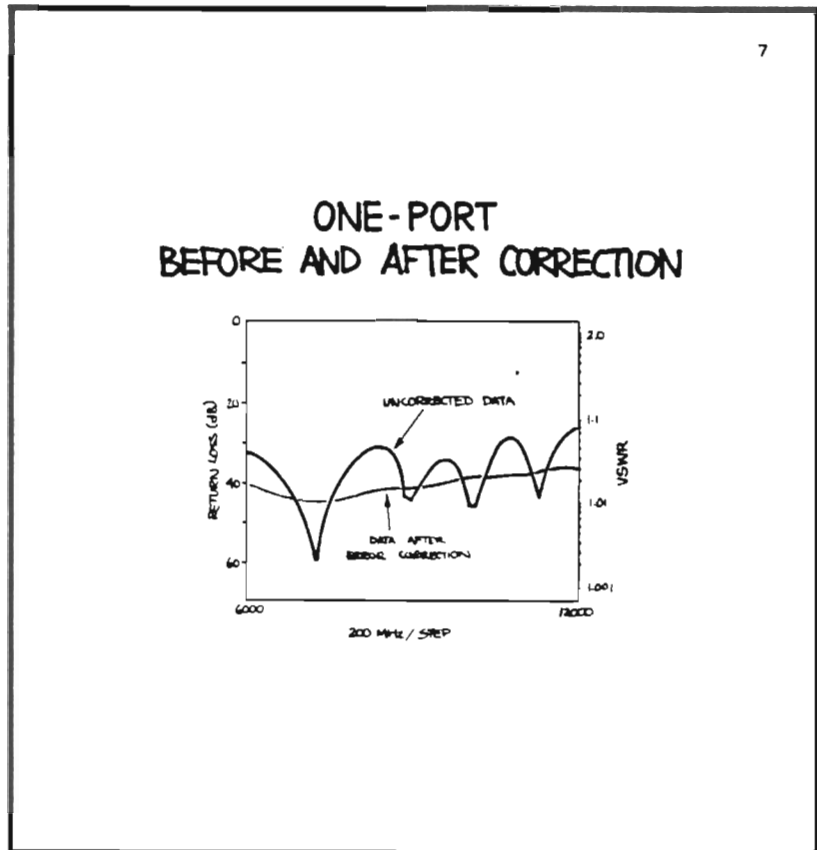


NOTE: SEE APPENDIX I FOR DETAILS

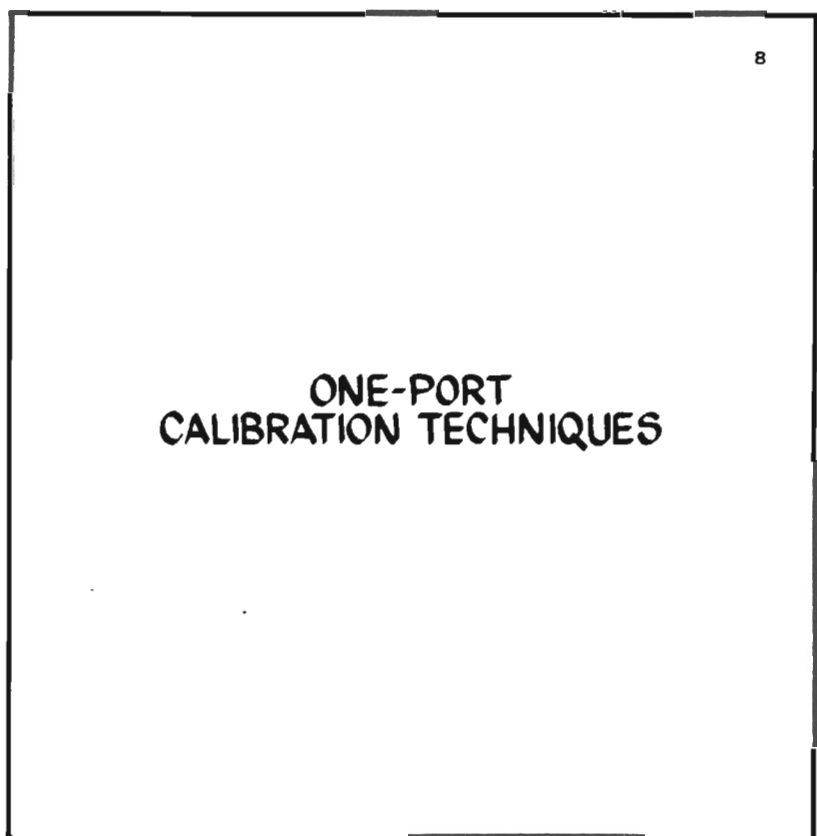
The flow graph of the fictitious two-port error adapter is connected to the unknown reflection coefficient ( $\Gamma_A$ ). A flow graph is a good way to give a practical feel for how signals are flowing in a microwave network. For example, suppose,  $\Gamma_A$  is a perfect  $Z_0$  termination. When  $\Gamma_M$  is measured, there are some residual signals caused by the system directivity  $e_{00}$ . This signal does not flow to the device under test but flows through the branch of the flow graph labeled  $e_{00}$ . The frequency response terms  $e_{10}$  and  $e_{01}$  can be best understood by measuring a short. A short has a reflection coefficient of -1 with no frequency response variations. But, due to the couplers, front-end mixers, cables, and other hardware there are definite frequency response variations modeled by the branches  $e_{10}$  and  $e_{01}$ . Looking back into the test port of the measurement system, it does not present a perfect  $Z_0$  source impedance. There is some reflection when a signal is incident on the test port. This is primarily due to the match of the couplers and/or adapters. The equivalent port match is modeled by the branch  $e_{11}$ .

$\Gamma_M$  is mathematically related to  $\Gamma_A$  by three error terms: directivity, frequency response, and port match. If these three terms are known from a calibration procedure, (discussed later), it is possible to solve for the actual reflection coefficient  $\Gamma_A$ .

This slide shows the return loss of a resistive termination before and after error correction. The directivity of the measurement system is about the same as the return loss of the resistive termination. 40 dB is a respectable equivalent directivity for a measurement system. But, at some frequencies, the directivity term adds in phase with the reflection coefficient of the actual device under test and yields a 6 dB higher measurement. At other frequencies, the directivity and reflection coefficient terms are out of phase and cancel, causing deep dips in the measurement data. Error correction does not remove all errors. Residual errors remaining in the measurement system may be due to imperfect standards, repeatability, noise, etc.. But the measurement accuracy is greatly improved. In fact, greater than 20 dB improvement is typical.



Having shown what error correction can accomplish, the problem of determining the error coefficients remains.



# ONE-PORT ERROR MODEL CALIBRATION

$$\Gamma_M = e_{00} + \frac{(e_{10} e_{01}) \Gamma_A}{1 - e_{11} \Gamma_A} \equiv \frac{a \Gamma_A + b}{c \Gamma_A + 1}$$

$$a = e_{10} e_{01} - e_{00} e_{11}$$

$$b = e_{00}$$

$$c = -e_{11}$$

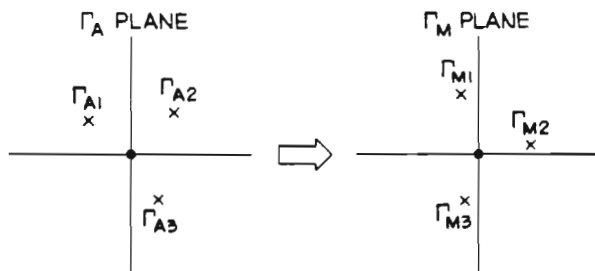
$$\Gamma_A a + b - \Gamma_A \Gamma_M c = \Gamma_M$$

- WITH 3 DIFFERENT KNOWN  $\Gamma_A$ , MEASURE THE RESULTANT 3  $\Gamma_M$
- THIS YIELDS 3 EQUATIONS TO SOLVE FOR a, b & c

$$\begin{aligned} \Gamma_{A1} a + b - \Gamma_{A1} \Gamma_{M1} c &= \Gamma_{M1} \\ \Gamma_{A2} a + b - \Gamma_{A2} \Gamma_{M2} c &= \Gamma_{M2} \\ \Gamma_{A3} a + b - \Gamma_{A3} \Gamma_{M3} c &= \Gamma_{M3} \end{aligned}$$

A process of calibration will now be discussed. By a change of variables, the equation for the measured reflection coefficient can be converted to a bilinear equation with the error terms a, b and c as variables. If there is a way to generate two more of these equations, giving three equations in the three unknowns, (a, b and c), then a system of equations results that can be solved for the error terms. The approach used in error correction for one-port networks is to measure three different known loads ( $\Gamma_A$ ). This generates three different measured reflection coefficients ( $\Gamma_M$ ). This procedure yields the necessary three equations to solve for the error terms a, b and c.

# BILINEAR TRANSFORMATION GENERAL CASE



$$\Gamma_M = \frac{a \Gamma_A + b}{c \Gamma_A + 1}$$

This is a graphic approach to the calibration technique. From complex algebra, if three points on the  $\Gamma_A$  plane and three points on the  $\Gamma_M$  plane are known, the terms a, b and c are uniquely determined for a bilinear transformation. This graphic approach will be helpful to visualize different calibration techniques.

These are four of the more popular calibration techniques. The first one basically goes back to the mathematical treatment of three different, known offset shorts for  $\Gamma_A$ . An offset short is a short circuit of precisely known length down an air line. The frequency must be known accurately to determine the phase shift at the offset short. The three offset shorts generate three equations to solve for the three unknown error terms. The phase of offset shorts is frequency sensitive. Therefore, care must be taken to avoid lengths that are multiples of a half-wavelength, or the offset shorts will not be unique. This technique is useful when dealing with microstrip and other transmission media where it is very difficult to realize  $Z_0$  loads or opens.

The second technique has been used for many years by Hewlett Packard on the large, computer-based, automatic network analyzers. The technique consists of using a  $Z_0$  termination, a good short circuit, and a series of offset shorts which are a quarter wavelength long in the center of the band to approximate an open circuit. It requires a series of offset shorts over the frequency range in order to approximate open circuits. The offset shorts are not broadband, but provide good accuracy.

The third technique is very similar to the second, but replaces the offset short with an open circuit. The open circuit has a fringing capacitance that needs to be modeled very precisely in order to achieve accuracy.

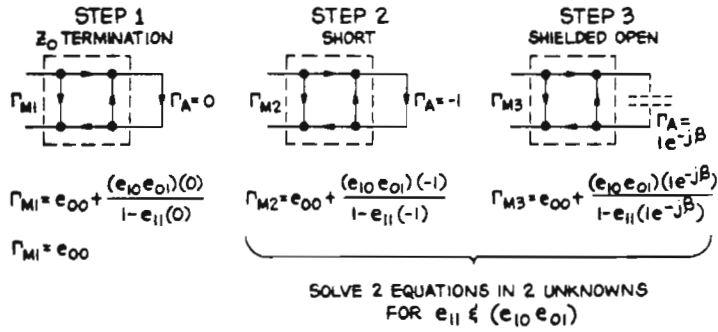
The last technique uses two different sliding terminations and a short circuit. This approach is the fussiest and the most mathematically involved, but has the potential of achieving the best performance.

The last two methods will now be discussed in detail.

## ONE-PORT CALIBRATION METHODS

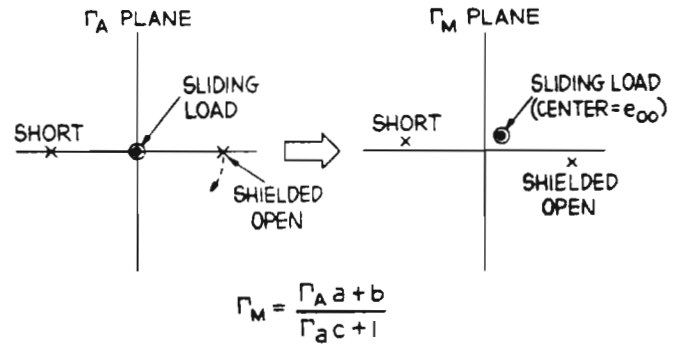
- 3 OR MORE DIFFERENT KNOWN OFFSET SHORTS
- $Z_0$  TERMINATION (FIXED OR SLIDING), SHORT, & OFFSET SHORT
- $Z_0$  TERMINATION (FIXED OR SLIDING), SHORT, & OPEN (CAPACITANCE MODELED)
- 2 DIFFERENT SLIDING TERMINATIONS & A SHORT

### ONE-PORT CALIBRATION USING $Z_0$ TERMINATION (FIXED OR SLIDING), SHORT & OPEN (CAPACITANCE MODELED)



The technique has three steps. First, attach a  $Z_0$  termination (notice,  $\Gamma_A = 0$ ) and measure  $\Gamma_{M1}$ . This yields the directivity term  $e_{00}$  directly. Next, connect a short and measure  $\Gamma_{M2}$ . The final step is to connect a shielded open and measure  $\Gamma_{M3}$ . Assume that the capacitance of the shielded open, which determines the phase term, is known. There are now two equations with two unknowns (the frequency response  $e_{10}e_{01}$ , and the port match  $e_{11}$ ) for which we can solve.

### BILINEAR TRANSFORMATION $Z_0$ TERMINATION (SLIDING), SHORT & OPEN (CAPACITANCE MODELED)



NOTE: SEE APPENDIX II FOR CIRCLE FITTING PROCEDURE

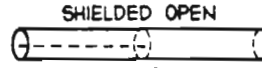
This is a graphic presentation of the preceding technique.

The short circuit is at -1 on the  $\Gamma_A$  plane, and the sliding load generates a circle, centered at the origin. The center of the circle is determined by the mechanical dimensions of the air line and yields an effective directivity of approximately 60 dB. The radius of the circle is determined by the residual reflection coefficient of the sliding element. As the sliding element is moved physically, it traces out the locus of a circle on the  $\Gamma_A$  plane. The open circuit at low frequencies is at +1 on the  $\Gamma_A$  plane, but as the frequency increases, the capacitive reactance starts to rotate the position of the shielded open clockwise. On the  $\Gamma_M$  plane the short's position is modified and the sliding load is no longer centered at the origin. The position of the shielded open is also modified.



The shielded open consists of an extension of the outer conductor of the coax beyond the termination of the inner conductor. This extension is a circular waveguide operating below its cut-off frequency. The impedance of such a waveguide section is reactive (a shunt capacitance) and cannot propagate power. The reflection coefficient of a shunt capacitor is  $e^{-j\beta}$ . Notice that  $j\beta$  is a function of frequency, so the frequency has to be known accurately as well as the value of the capacitance. The capacitance of a waveguide increases the closer you get to the cut-off frequency. We can model this capacitance as a power series and determine empirically the power series coefficients. Notice that the capacitance rises approximately 15% at 18 GHz.

## OPEN CAPACITANCE MODEL



$$\Gamma_A = 1e^{-j\beta}$$

$$\beta = 2 \tan^{-1} 2\pi f C Z_0$$

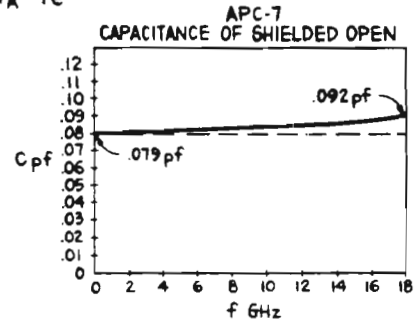
$$C \cong C_0 + C_1 f + C_2 f^2$$

FOR APC-7:

$$C_0 = .079 \text{ pf}$$

$$C_1 = 0 \text{ pf/Hz}$$

$$C_2 = 4.0 \times 10^{-23} \text{ pf/Hz}^2$$

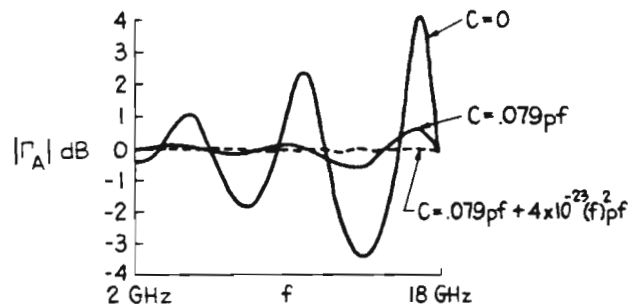


NOTE: SEE APPENDIX III FOR DETAILS

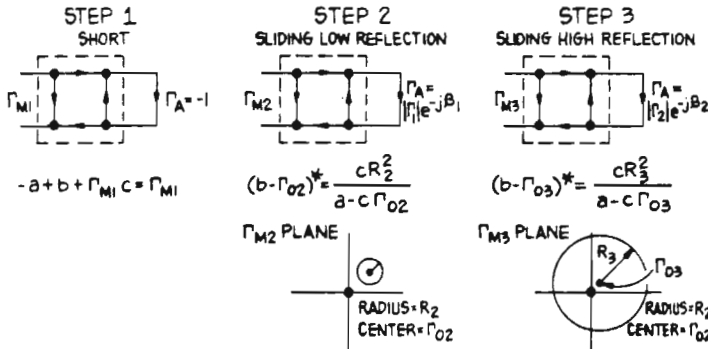
This slide shows the results of measuring the reflection coefficient of an APC-7 offset short using the open capacitance model. With the capacitance equal to zero, there is approximately an 8 dB peak-to-peak error, showing that a simple open circuit is not a good model for high frequency calibration. If the dc capacitance term is modeled, the error can be reduced to approximately 1 dB peak-to-peak error. By modeling the capacitance as a function of frequency, the error is reduced to less than .1 dB peak-to-peak.

## RESULTS USING OPEN CAPACITANCE MODEL

APC-7 OFFSET SHORT



### ONE-PORT CALIBRATION USING 2 DIFFERENT SLIDING TERMINATIONS & A SHORT



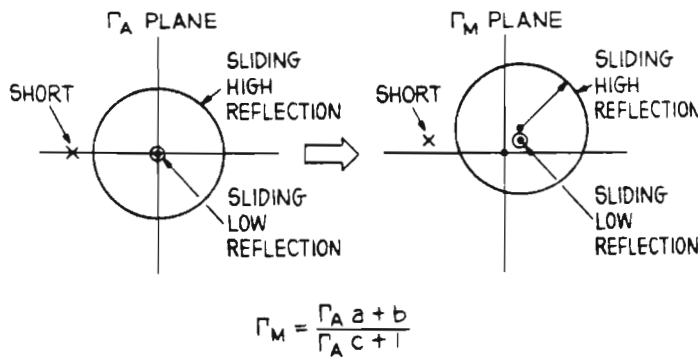
SOLVE 3 EQUATIONS IN 3 UNKNOWNNS  
 NOTE: SEE APPENDIX IV FOR DETAILS

This second procedure shows how to use two different sliding terminations and a short circuit for calibration. Step 1 connects a short circuit on the test port and measures  $\Gamma_{M1}$ . Step 2 uses a sliding, low reflection termination to define a circle on the  $\Gamma_M$  plane with the center at  $\Gamma_{O2}$  and the radius  $R_2$ . Step 3 connects a high reflection sliding termination to define a second circle with the center  $\Gamma_{O3}$  and radius  $R_3$ . Steps 1 through 3 yield three equations which can be solved for the three unknowns: a, b, and c. The center and radius of the two circles can be determined by a circle fitting technique.

It should be noted that certain assumptions have been made about the sliding terminations:  
 (1) The magnitude of the reflection coefficient cannot change as it rotates in phase.  
 (2) Air line loss is negligible.

This technique does not require an accurate knowledge of the frequency. The magnitude and phase of the sliding terminations are also not needed. This technique can be very accurate, but it is more time consuming and not nearly as easy to apply as the previous approach.

### BILINEAR TRANSFORMATION 2 DIFFERENT SLIDING TERMINATIONS & A SHORT



This graphically shows how the circles on the  $\Gamma_A$  plane are modified when they are transformed to the  $\Gamma_M$  plane.

In conclusion, this section demonstrates that with one-port error correction, the system directivity is extended, response errors are reduced significantly, and port match uncertainties are lowered. Calibration makes a marked improvement when measuring with adapters and cables since their effects are removed. The use of cables requires care because their characteristics change as they are flexed. If semi-rigid coax is used, is carefully positioned, and remains stationary, then the errors due to these lines can be greatly reduced, offering alternative ways to connect to the device under test.

18

## CONTRIBUTIONS OF ONE-PORT ERROR CORRECTION

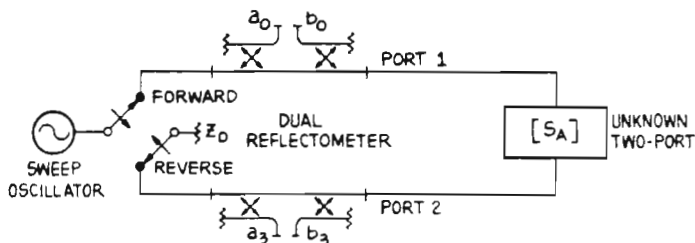
- EXTENDS SYSTEM DIRECTIVITY
- REDUCES FREQUENCY RESPONSE ERRORS
- LOWERS PORT MATCH UNCERTAINTIES
- LESSENS EFFECT OF ADAPTERS & CABLES

Accuracy enhancement techniques for two-port networks will now be discussed. The presentation will follow the same development as the prior one-port case.

19

## ACCURACY ENHANCEMENT FOR TWO-PORT NETWORKS

## THE PROBLEM TWO-PORT

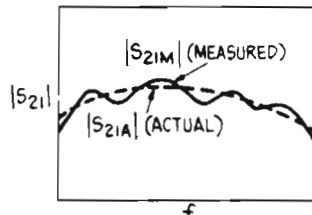


$$S_{11M} = \frac{b_0}{a_0}, \text{ OSC SWITCHED FORWARD}$$

$$S_{21M} = \frac{b_3}{a_0}, \text{ OSC SWITCHED FORWARD}$$

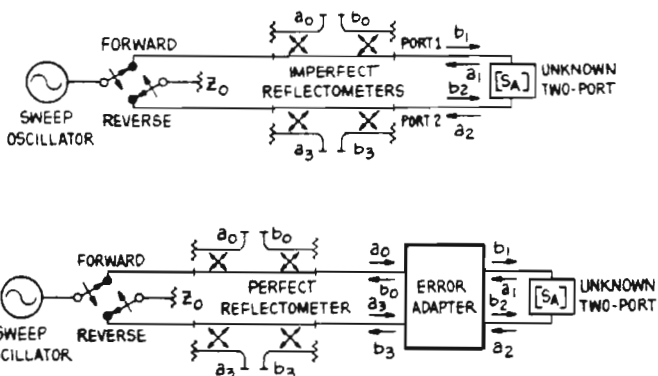
$$S_{22M} = \frac{b_3}{a_3}, \text{ OSC SWITCHED REVERSE}$$

$$S_{12M} = \frac{b_0}{a_3}, \text{ OSC SWITCHED REVERSE}$$



The two-port measurement system duplicates part of the one-port measurement system discussed earlier. A dual directional coupler is attached to the input of the unknown two-port, and another dual directional coupler is attached to the output. A switch changes the direction of the incident power to the unknown two-port for forward and reverse measurements and terminates the unknown two-port in an impedance  $Z_0$ . The problems are very similar to those of the one-port case. There are directivity errors, frequency response errors, and port match errors, for both ports. For example, the dotted line in the graph represents the actual frequency response of a device; The solid line represents the measured result. Again, it is not the device but the measurement system causing the error.

## TWO-PORT ERROR MODEL (WITH 4 MEASUREMENT PORTS)

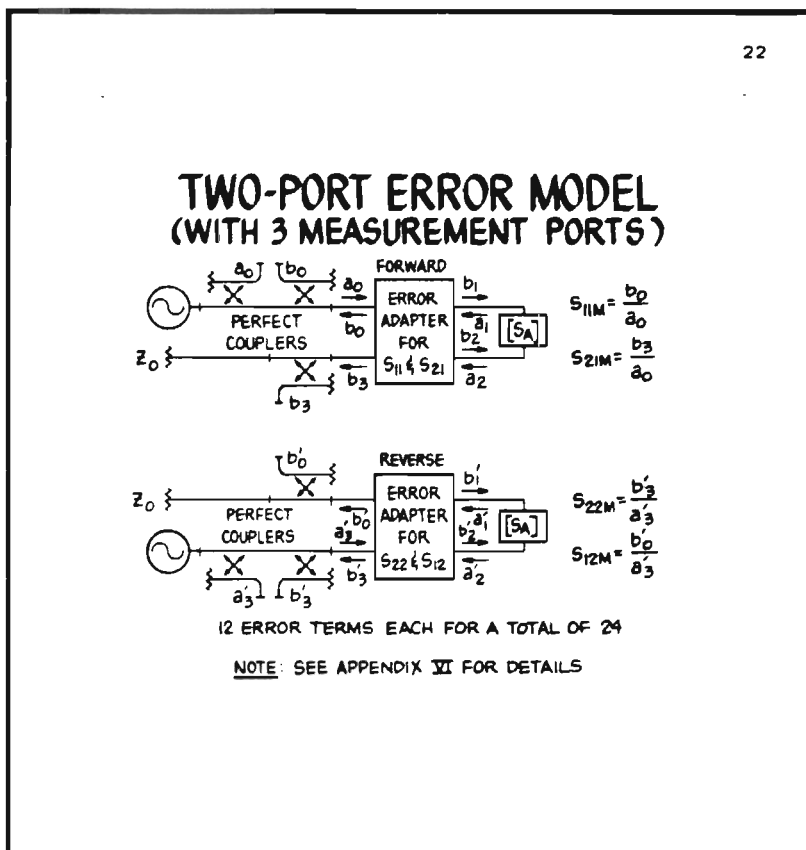


16 ERROR TERMS  
NOTE: SEE APPENDIX V FOR DETAILS

Paralleling the previous one-port analysis, all the linear errors of the imperfect reflectometer can be combined into an error adapter. In this case, the fictitious error adapter must be a four-port. This error adapter has 16 error terms. The number of error terms is the square of the number of ports.

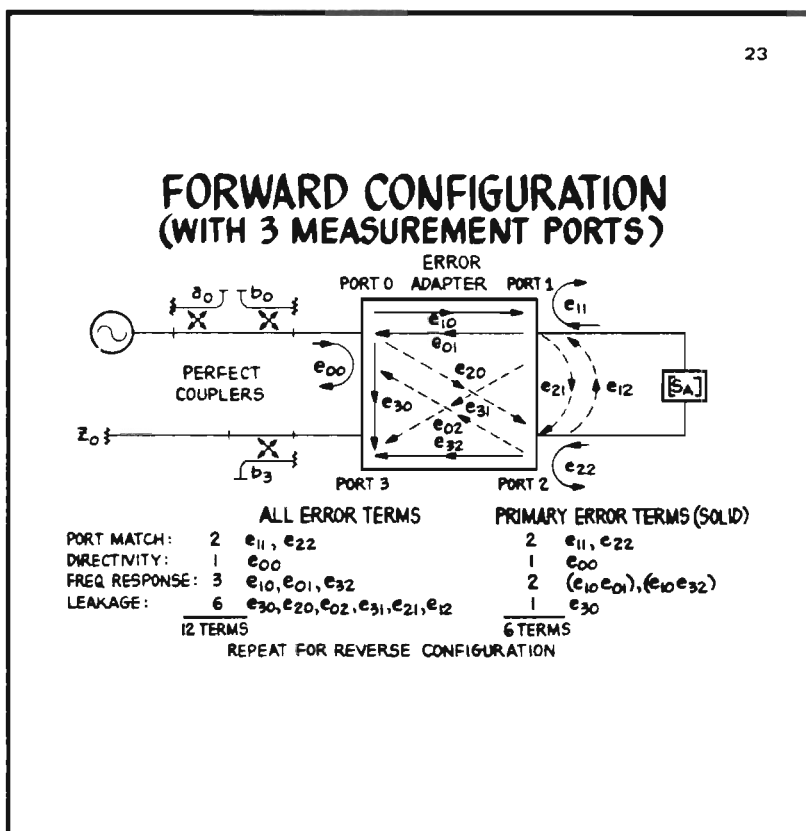
There are additional problems because the error adapter does not include switch repeatability errors, or changing port match due to different switch positions. Errors caused by the switch can be removed by a procedure that will be discussed later. To resolve further difficulties, one of the following assumptions must be made. (1) There are four samplers or mixers which can be connected at all times to the four measurement ports of the couplers. Otherwise, additional switches would need to be included in the model. (2) If additional switches are included, an assumption could be made that the isolation of the couplers is high enough to reduce the errors caused by this additional switching.

Here is another approach to the same measurement problem. A fictitious error adapter has been created for the forward direction with the source and the load connected in the proper position. There are only three measurement ports. There is another separate error adapter for the reverse direction. By using two separate error adapters, the switch problems and the necessity of having four measurement ports has been removed. This is a typical model used widely in error correction techniques. Each one of these error adapters has 12 error terms. So, there is a total of 24. Two of the questions that arise are: Are all of the error terms meaningful? And, what is the physical description of each of the error terms? These will be discussed next.

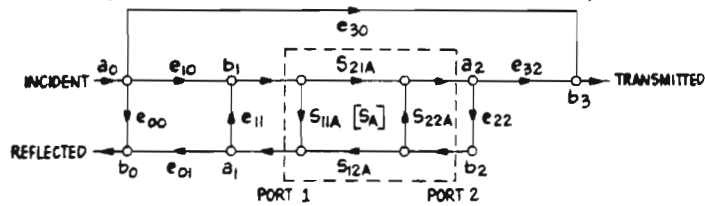


This is a pictorial flow graph indicating the error terms for the forward configuration. As mentioned earlier, there are 12 error terms. There are two port match terms ( $e_{11}$  and  $e_{22}$ ) and a directivity term ( $e_{00}$ ). For the frequency response, there are:  $e_{10}$  and  $e_{01}$  for making reflection measurements and  $e_{10}$  and  $e_{32}$  for transmission measurements. The remaining six terms are leakage terms between the various ports.

For a typical S-parameter test set using high directivity couplers with good isolation, the primary terms are indicated by the solid lines and the less important terms by the dotted lines. The primary errors are: The two-port match errors ( $e_{11}$  and  $e_{22}$ ); The directivity error ( $e_{00}$ ); The frequency response errors (the reflection frequency response term  $e_{10}$  and the transmission frequency response term  $e_{10}$   $e_{32}$ ); and the leakage term ( $e_{30}$ ). These are the six complex error terms for the forward direction. The procedure can be repeated for the reverse configuration to obtain six additional error terms. This leads to the "twelve term error model".



## TWO-PORT FORWARD FLOW GRAPH (WITH 3 MEASUREMENT PORTS)



PORT 1 MATCH:  $e_{11}$       TRANS FREQ RESPONSE:  $(e_{10}e_{32})$   
 PORT 2 MATCH:  $e_{22}$       DIRECTIVITY:  $e_{00}$   
 REFL FREQ RESPONSE:  $(e_{10}e_{01})$       LEAKAGE:  $e_{30}$

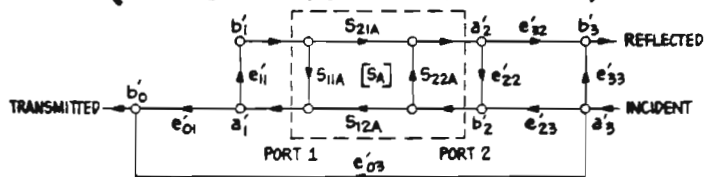
$$S_{11M} = \frac{b_0}{a_0} = e_{00} + (e_{10}e_{01}) \frac{S_{11A} - e_{22} \text{DET}[S_A]}{1 - e_{11}S_{11A} - e_{22}S_{22A} + e_{11}e_{22} \text{DET}[S_A]}$$

$$S_{21M} = \frac{b_3}{a_0} = e_{30} + (e_{10}e_{32}) \frac{S_{21A}}{1 - e_{11}S_{11A} - e_{22}S_{22A} + e_{11}e_{22} \text{DET}[S_A]}$$

NOTE: SEE APPENDIX VIII FOR DETAILS       $\text{DET}[S_A] = S_{11A}S_{22A} - S_{21A}S_{12A}$

This is a flow graph for the forward configuration with the assumptions that were made on the previous slide. Note that  $S_{11M}$  and  $S_{21M}$  are functions of all four S-parameters of the device under test  $[S_A]$ .

## TWO-PORT REVERSE FLOW GRAPH (WITH 3 MEASUREMENT PORTS)



PORT 1 MATCH:  $e_{11}$       TRANS FREQ RESPONSE:  $(e'_{23}e'_{01})$   
 PORT 2 MATCH:  $e_{22}$       DIRECTIVITY:  $e'_{33}$   
 REFL FREQ RESPONSE:  $(e'_{23}e'_{32})$       LEAKAGE:  $e'_{03}$

$$S_{22M} = \frac{b'_3}{a'_3} = e'_{33} + e'_{23}e'_{32} \frac{S_{22A} - e'_{11} \text{DET}[S_A]}{1 - e'_{11}S_{11A} - e'_{22}S_{22A} + e'_{11}e'_{22} \text{DET}[S_A]}$$

$$S_{12M} = \frac{b'_0}{a'_3} = e'_{03} + e'_{23}e'_{01} \frac{S_{12A}}{1 - e'_{11}S_{11A} - e'_{22}S_{22A} + e'_{11}e'_{22} \text{DET}[S_A]}$$

NOTE: SEE APPENDIX VIII FOR DETAILS       $\text{DET}[S_A] = S_{11A}S_{22A} - S_{21A}S_{12A}$

This is a flow graph of the reverse configuration. Note again, that the measured S-parameters are functions of all the S-parameters of the device under test.

Four measurements have been made: The S-parameters  $S_{11M}$ ,  $S_{21M}$ ,  $S_{12M}$  and  $S_{22M}$ . Each of these measured S-parameters is a function of the four S-parameters of the device under test plus 12 error terms. Now, if these error terms can be determined by a calibration procedure, (described later), four equations in the four unknowns  $S_{11A}$ ,  $S_{21A}$ ,  $S_{22A}$  and  $S_{12A}$  result. This system of equations can be solved for the actual S-parameters. Notice that the  $S_{21A}$  transmission coefficient is a function not only of the measured  $S_{21M}$  but of the other three S-parameters as well. It takes four measurements to calculate one S-parameter.

## SOLVING FOR [S<sub>A</sub>] (WITH 3 MEASUREMENT PORTS)

- FORWARD  $S_{11M}$  = FUNCTION OF [ $S_{11A}$ ,  $S_{21A}$ ,  $S_{12A}$ ,  $S_{22A}$ ,  $e_{11}$ ,  $e_{22}$ , ( $e_{10} e_{01}$ ) &  $e_{00}$ ]  
 $S_{21M}$  = FUNCTION OF [ $S_{11A}$ ,  $S_{21A}$ ,  $S_{12A}$ ,  $S_{22A}$ ,  $e_{11}$ ,  $e_{22}$ , ( $e_{10} e_{32}$ ) &  $e_{30}$ ]  
 REVERSE  $S_{22M}$  = FUNCTION OF [ $S_{11A}$ ,  $S_{21A}$ ,  $S_{12A}$ ,  $S_{22A}$ ,  $e'_{11}$ ,  $e'_{22}$ , ( $e'_{23} e'_{32}$ ) &  $e'_{33}$ ]  
 $S_{12M}$  = FUNCTION OF [ $S_{11A}$ ,  $S_{21A}$ ,  $S_{12A}$ ,  $S_{22A}$ ,  $e'_{11}$ ,  $e'_{22}$ , ( $e'_{23} e'_{01}$ ) &  $e'_{03}$ ]
- IF WE KNOW THE ERROR TERMS BY CALIBRATION
  - THEN WE HAVE 4 EQUATIONS IN 4 UNKNOWNNS
  - SOLVE SIMULTANEOUSLY TO YIELD  $S_{11A}$ ,  $S_{21A}$ ,  $S_{12A}$  &  $S_{22A}$

$$S_{21A} = \frac{\left(\frac{S_{21M} - e_{30}}{e_{10} e_{32}}\right) \left[1 + \left(\frac{S_{22M} - e'_{33}}{e'_{23} e'_{32}}\right) (e'_{22} - e_{22})\right]}{\left(1 + \frac{S_{11M} - e_{00}}{e_{10} e_{01}} e_{11}\right) \left(1 + \frac{S_{22M} - e'_{33}}{e'_{23} e'_{32}} e'_{22}\right) - \left(\frac{S_{21M} - e_{30}}{e_{10} e_{32}}\right) \left(\frac{S_{12M} - e'_{03}}{e'_{23} e'_{01}}\right) e_{22} e'_{11}}$$

NOTE: SEE APPENDIX VIII FOR DETAILS

Here are the solutions for the remaining actual S-parameters of the device under test.

## SOLVING FOR [S<sub>A</sub>] CONT'D (WITH 3 MEASUREMENT PORTS)

$$S_{11A} = \frac{\left(\frac{S_{11M} - e_{00}}{e_{10} e_{01}}\right) \left(1 + \frac{S_{22M} - e'_{33}}{e'_{23} e'_{32}} e'_{22}\right) - e_{22} \left(\frac{S_{21M} - e_{30}}{e_{10} e_{32}}\right) \left(\frac{S_{12M} - e'_{03}}{e'_{23} e'_{01}}\right)}{D}$$

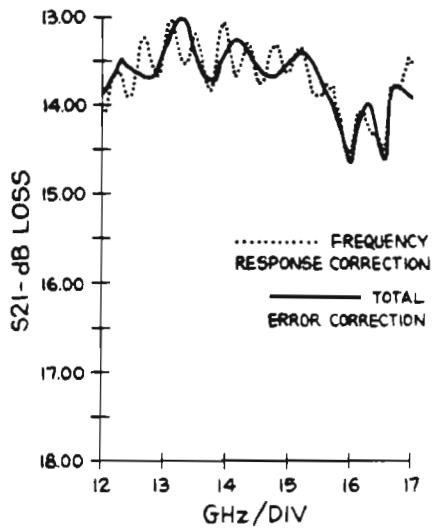
$$S_{12A} = \frac{\left(\frac{S_{12M} - e'_{03}}{e'_{23} e'_{01}}\right) \left[1 + \left(\frac{S_{11M} - e_{00}}{e_{10} e_{01}}\right) (e_{11} - e'_{11})\right]}{D}$$

$$S_{22A} = \frac{\left(\frac{S_{22M} - e'_{33}}{e'_{23} e'_{32}}\right) \left(1 + \frac{S_{11M} - e_{00}}{e_{10} e_{01}} e_{11}\right) - e'_{11} \left(\frac{S_{21M} - e_{30}}{e_{10} e_{32}}\right) \left(\frac{S_{12M} - e'_{03}}{e'_{23} e'_{01}}\right)}{D}$$

$$D = \left(1 + \frac{S_{11M} - e_{00}}{e_{10} e_{01}} e_{11}\right) \left(1 + \frac{S_{22M} - e'_{33}}{e'_{23} e'_{32}} e'_{22}\right) - \left(\frac{S_{21M} - e_{30}}{e_{10} e_{32}}\right) \left(\frac{S_{12M} - e'_{03}}{e'_{23} e'_{01}}\right) e_{22} e'_{11}$$

NOTE: SEE APPENDIX VIII FOR DETAILS

### TWO-PORT BEFORE AND AFTER CORRECTION FOR A MISMATCHED PAD



This slide shows the magnitude  $S_{21}$  for a "mismatched pad." The dotted line is the corrected data with only the frequency response errors removed. The solid line shows the corrected data when using the 12 term error model. By including the error terms  $e_{11}$  and  $e_{22}$ , the .5dB peak-to-peak error is reduced significantly.

### TWO-PORT CALIBRATION TECHNIQUES

The theory of error correction for two-port networks has been developed. It now remains to develop the solutions for the various error terms.



Two calibration techniques will be discussed in detail. One is a standard calibration technique that has been used for many years at Hewlett Packard. The other is a self-calibration technique where precise knowledge of the standards is not required.

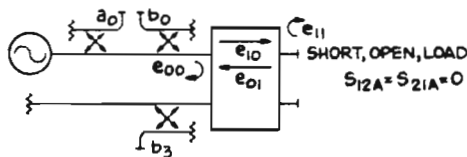
## TWO-PORT CALIBRATION TECHNIQUES

- I. STANDARD CALIBRATION PROCEDURE
- II. SELF-CALIBRATION PROCEDURE

Step (1) of the standard calibration procedure is to calibrate port 1 using the one-port procedure that was developed earlier. Place a short, an open, and a load on port 1 and solve for the three error terms: the equivalent directivity ( $e_{00}$ ), the port match ( $e_{11}$ ), and the reflection frequency response ( $e_{10}, e_{01}$ ). When one-port devices are used on the two-port measurement system, the equation for the reflection coefficient of the two-port case reduces to that of the one-port case.

### STANDARD CALIBRATION PROCEDURE (FORWARD CONFIGURATION WITH 3 MEASUREMENT PORTS)

STEP 1: CALIBRATE PORT 1 USING ONE-PORT PROCEDURE

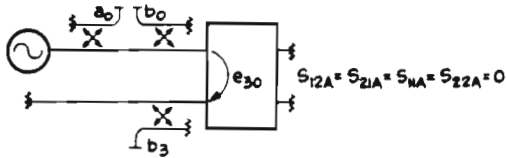


$$\bullet S_{NM} = \frac{b_0}{a_0} = e_{00} + (e_{10}e_{01}) \frac{S_{11A} - e_{22} \text{DET}[S_A]}{1 - e_{11}S_{11A} - e_{22}S_{22A} + e_{11}e_{22} \text{DET}[S_A]} \rightarrow e_{00} + (e_{10}e_{01}) \frac{S_{11A}}{1 - e_{11}S_{11A}}$$

- USE ANY OF THE FOUR APPROACHES DESCRIBED IN THE ONE-PORT CALIBRATION SECTION
- SOLVE FOR:  $e_{00}, e_{11} \& (e_{10}e_{01})$

## STANDARD CALIBRATION PROCEDURE (FORWARD CONFIGURATION WITH 3 MEASUREMENT PORTS)

STEP 2: CONNECT  $Z_0$  TERMINATIONS TO PORTS 1 & 2

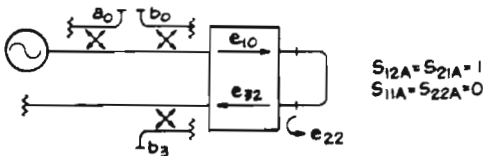


- $S_{21M} = \frac{b_3}{a_0} = e_{30} + (e_{10} e_{32}) \frac{S_{21A}}{1 - e_{11} S_{11A} - e_{22} S_{22A} + e_{11} e_{22} \text{DET}[S_A]} \rightarrow e_{30}$
- $e_{30} = S_{21M}$

Step (2) is to determine the leakage. This can be accomplished by placing  $Z_0$  terminations on port 1 and port 2. In this case, the equation for  $S_{21M}$  is equal to the leakage term  $e_{30}$ .

## STANDARD CALIBRATION PROCEDURE (FORWARD CONFIGURATION WITH 3 MEASUREMENT PORTS)

STEP 3: CONNECT PORTS 1 & 2 TOGETHER



- $S_{NM} = \frac{b_0}{a_0} \rightarrow e_{00} + (e_{10} e_{01}) \frac{e_{22}}{1 - e_{11} e_{22}}$
- WE KNOW  $e_{00}$ ,  $e_{11}$  &  $(e_{10} e_{01})$  ∴ SOLVE FOR  $e_{22}$
- $S_{21M} = \frac{b_3}{a_0} \rightarrow e_{30} + (e_{10} e_{32}) \frac{1}{1 - e_{11} e_{22}}$
- WE KNOW  $e_{30}$ ,  $e_{11}$  &  $e_{22}$  ∴ SOLVE FOR  $(e_{10} e_{32})$

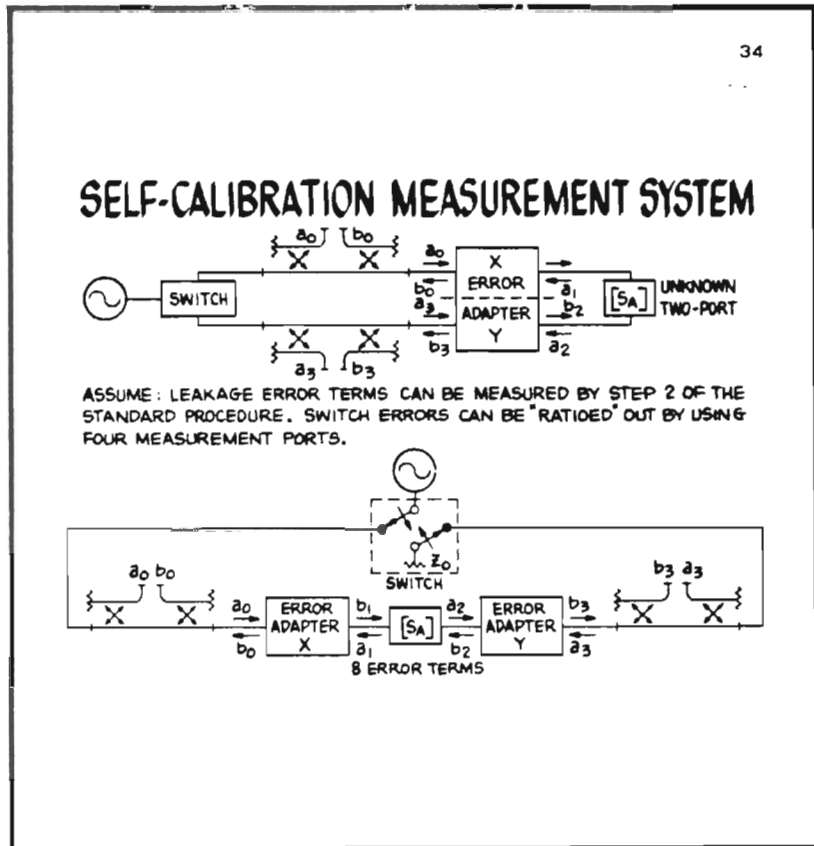
REPEAT FOR REVERSE CONFIGURATION

Step (3) is to connect port 1 and port 2 of the measurement system together. This reduces the equation for  $S_{21M}$  to an equation for a one-port measurement system. Since the three error terms for port 1 were previously determined, the one-port measurement system can now be used to measure the port match of port 2 ( $e_{22}$ ).

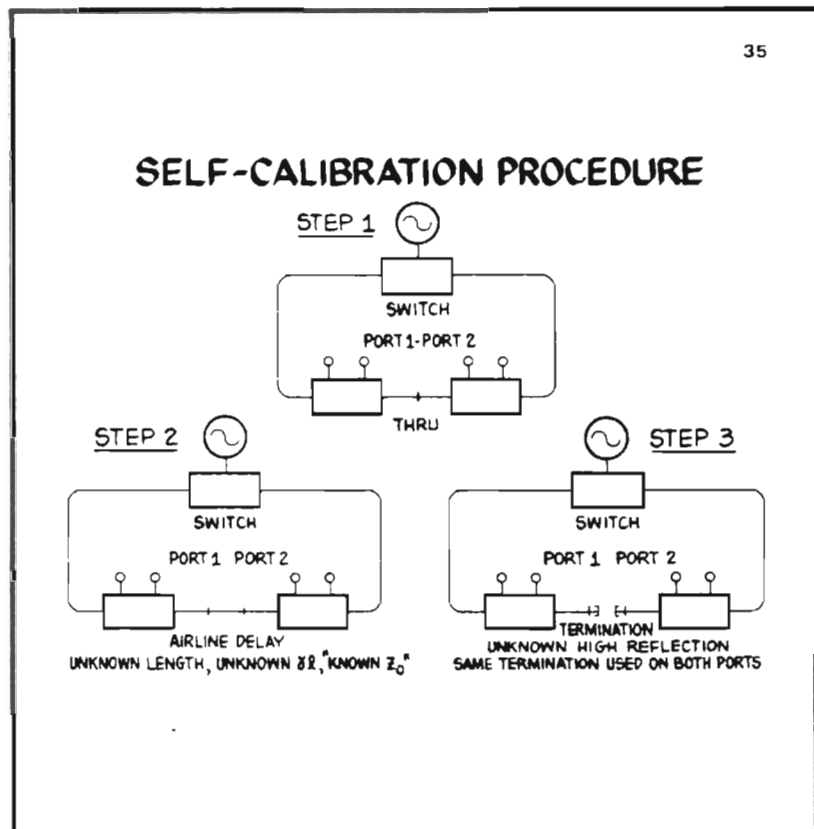
$S_{21M}$  reduces to a simple expression for the thru connection. The leakage term ( $e_{30}$ ) has been determined and the two port matches ( $e_{11}$  and  $e_{22}$ ) are known, so the remaining transmission frequency response term ( $e_{10} e_{32}$ ) can be easily solved.

This procedure can be repeated for the reverse direction to determine the remaining six error terms. It should be noted that with this calibration procedure, it is necessary to know the  $Z_0$  termination accurately. It is also necessary to have a good short and to know the open circuit capacitance effects accurately. However, it is a very straight-forward procedure when characteristics of the standards are known.

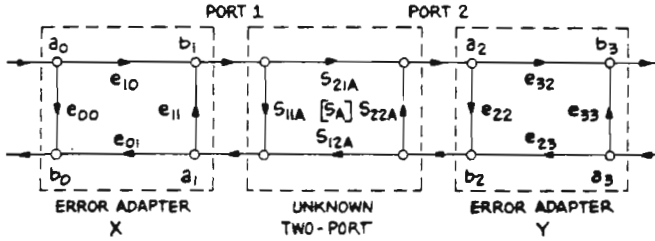
The self-calibration technique requires very little knowledge about the standards. Assume the leakage error terms can be measured by Step (2) of the standard calibration procedure described earlier. The error adapter can then be separated into an X-error adapter and a Y-error adapter, and there will be no leakage between adapters. The switching errors can be removed by a technique to be described later. Then the measurement system can be modified so that it has an error adapter (X) on the port 1 side and an error adapter (Y) on the port 2 side of the device under test. This measurement approach uses eight error terms.



The self-calibration technique is a three step procedure. Step (1), connect the two ports together (thru connection) and measure the four S-parameters; Step (2), connect an air line delay of unknown length and unknown propagation constant (but known  $Z_0$ ) and make four more S-parameter measurements; Step (3), connect an unknown high reflection termination, an open or short for example, to port 1 and port 2, and make the two reflection measurements. A total of ten measurements has now been made. Only eight unknown error terms need to be determined. The redundant information can be used to calculate the propagation constant of the air line and the reflection coefficient of the high reflection termination that was placed on the system in Step (3).



## ERROR MODEL FOR SELF-CALIBRATION



### CASCADE PARAMETERS

$$\begin{bmatrix} b_0 \\ a_0 \end{bmatrix} = [T_X] \begin{bmatrix} a_1 \\ b_1 \end{bmatrix}, \quad \begin{bmatrix} a_1 \\ b_1 \end{bmatrix} = [T_A] \begin{bmatrix} a_2 \\ b_2 \end{bmatrix}, \quad \begin{bmatrix} b_2 \\ a_2 \end{bmatrix} = [T_Y] \begin{bmatrix} a_3 \\ b_3 \end{bmatrix}$$

$$\therefore [T_M] = [T_X] [T_A] [T_Y]$$

NOTE: SEE APPENDIX VIII FOR DETAILS

A flow graph can be drawn for the measurement system with the error adapter X, the unknown two-port, and the error adapter Y. S-parameters can be used to solve this system. However, it is mathematically more convenient to use cascade parameters or T-parameters because the overall measured T-parameter matrix is simply a multiplication of the individual T-parameter matrices.

## THRU AND DELAY CONNECTION FOR SELF-CALIBRATION

STEP 1  
THRU CONNECTION

$$[T_{AT}] = \begin{bmatrix} 1 & 0 \\ 0 & 1 \end{bmatrix}$$

$$[T_{MT}] = [T_X] [T_Y]$$

STEP 2  
AIRLINE DELAY CONNECTION

$$[T_{AD}] = \begin{bmatrix} e^{-\gamma l} & 0 \\ 0 & e^{\gamma l} \end{bmatrix}$$

$$[T_{MD}] = [T_X] [T_{AD}] [T_Y]$$

THE ABOVE TWO MATRIX EQUATIONS CAN BE SOLVED FOR:

$$\gamma l, e_{00}, e_{33}, \frac{(e_{10} e_{01})}{e_{11}} \text{ \& } \frac{(e_{23} e_{32})}{e_{22}}$$

NOTE: SEE APPENDIX VIII FOR DETAILS

Step (1) is the thru connection. Notice that the T-parameters of the thru connection  $[T_{AT}]$  is the identity matrix. Step (2) is the delay connection. For the delay connection, the T-parameters  $[T_{AD}]$  also form a diagonal matrix since the air line is assumed non-reflective. The length and loss of the air line are defined by  $\gamma l$ . The four S-parameters are measured for the thru and delay connection, then transformed to T-parameters. The two resultant matrix equations  $[T_{MT}]$  and  $[T_{MD}]$  can then be solved for the directivity terms ( $e_{00}$  and  $e_{33}$ ), the propagation constant ( $\gamma l$ ) of the air line, and two terms that are the ratio of the frequency responses ( $e_{10} e_{01}$ ) and ( $e_{23} e_{32}$ ) to port match  $e_{11}$  and  $e_{22}$ . The port match terms  $e_{11}$  and  $e_{22}$  will be determined next.

Step (3) is to solve for the two port match terms ( $e_{11}$  and  $e_{22}$ ) by using an unknown termination ( $\Gamma_A$ ). First, place the termination on port 1 and measure the reflection coefficient ( $\Gamma_{MX}$ ); then place  $\Gamma_A$  on port 2 and measure  $\Gamma_{MY}$ . During the thru connection, use the port 1 reflectometer to measure the port match  $e_{22}$  yielding  $\Gamma_{M1}$ . These three equations can be solved for the two port matches ( $e_{11}$  and  $e_{22}$ ) and the reflection coefficient of the unknown termination ( $\Gamma_A$ ). The directivity, the frequency response, and the port match have now been determined for both reflectometers. The propagation constant ( $\gamma l$ ) of the air line and the unknown termination ( $\Gamma_A$ ) have also been determined. It is still necessary to determine the frequency response terms ( $e_{10}$ ,  $e_{32}$  and  $e_{23}$ ,  $e_{01}$ ) in transmission. This can be done using Step (3) of the standard calibration procedure described earlier.

38

### TERMINATION CONNECTION FOR SELF-CALIBRATION

STEP 3: SOLVE FOR  $e_{11}$  AND  $e_{22}$  USING TERMINATION

<p style="text-align: center;">UNKNOWN REFLECTION (<math>\Gamma_A</math>) ON PORT 1</p> $\Gamma_{MX} = e_{00} + \frac{(e_{10}e_{01})\Gamma_A}{1 - e_{11}\Gamma_A}$ <p style="text-align: center;">SOLVE FOR <math>\Gamma_A</math> IN TERMS OF <math>e_{11}</math></p>	<p style="text-align: center;">THRU</p> $\Gamma_{M1} = e_{00} + \frac{(e_{10}e_{01})e_{22}}{1 - e_{11}e_{22}}$ <p style="text-align: center;">SOLVE FOR <math>e_{11}</math> IN TERMS OF <math>e_{22}</math></p>	<p style="text-align: center;">UNKNOWN REFLECTION (<math>\Gamma_A</math>) ON PORT 2</p> $\Gamma_{MY} = e_{33} + \frac{(e_{23}e_{32})\Gamma_A}{1 - e_{22}\Gamma_A}$ <p style="text-align: center;">SOLVE FOR <math>\Gamma_A</math> IN TERMS OF <math>e_{22}</math></p>
---	---	---

THE ABOVE THREE EQUATIONS SOLVED FOR:

$\Gamma_A, e_{11} \text{ \& } e_{22}$

USE STANDARD CALIBRATION PROCEDURE STEP 3 TO SOLVE:

$(e_{10}e_{32}) \text{ \& } (e_{23}e_{01})$

NOTE: SEE APPENDIX VIII FOR DETAILS

An air line does not have shunt losses. Therefore, the  $Z_0$  is defined as  $\gamma l / j\omega C l$ . The propagation constant ( $\gamma l$ ) was calculated as part of the calibration procedure. So, the only unknown remaining is the total capacitance of the air line ( $C l$ ). This capacitance is determined by actual physical dimensions of the air line. These physical dimensions become the standard.

39

### $Z_0$ OF UNKNOWN AIR LINE FOR SELF-CALIBRATION

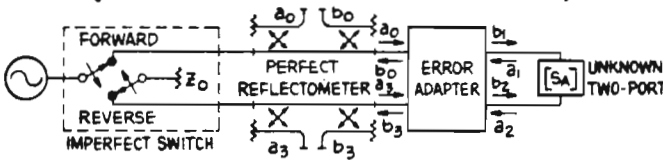
IF NO SHUNT LOSSES:

$$Z_0 = \frac{\gamma l}{j\omega C l}$$

WE CALCULATED  $\gamma l$

NEED ONLY KNOW  $C l$  !!

## REMOVAL OF SWITCHING ERRORS (WITH 4 MEASUREMENT PORTS)



### FORWARD

$$b_0 = S_{11M} a_0 + S_{12M} a_3$$

$$b_3 = S_{21M} a_0 + S_{22M} a_3$$

### REVERSE

$$b'_0 = S_{11M} a'_0 + S_{12M} a'_3$$

$$b'_3 = S_{21M} a'_0 + S_{22M} a'_3$$

SOLVING THE ABOVE SET OF EQUATIONS YIELDS :

IMPERFECT SWITCH IS "RATIOED" OUT	$S_{11M} = \frac{b_0 a'_3 - b'_0 a_3}{a_0 a'_3 - a_3 a'_0}$	$S_{12M} = \frac{b'_0 a_0 - b_0 a'_0}{a_0 a'_3 - a_3 a'_0}$	NOTE: SEE APPENDIX IX FOR DETAILS
	$S_{21M} = \frac{b_3 a'_3 - b'_3 a_3}{a_0 a'_3 - a_3 a'_0}$	$S_{22M} = \frac{b'_3 a_0 - b_3 a'_0}{a_0 a'_3 - a_3 a'_0}$	

It has been mentioned many times that it is necessary to remove the switching errors. Typically, when S-parameters are measured, the ports are terminated with a  $Z_0$  termination, and the S-parameters are measured as a simple ratio of the reflected to incident signal, etc.. However, it is just as valid to measure the S-parameter when a network is not terminated in its  $Z_0$  impedance. It simply takes more measurements. A set of S-parameter equations can be written for the forward direction and a set of S-parameter equations for the reverse direction. This procedure generates four equations that can be solved for the measured S-parameters. This yields the general equations for the S-parameters if the system has not been terminated with  $Z_0$  impedances. The above technique eliminates the effect of the switch. It does this in a practical sense by "ratioing out" the switch errors. For example, the source errors are "ratioed out" with the two reflectometers on the source side, and the load errors are "ratioed out" with the two reflectometers on the load side. Notice that the equations simplify back to the standard form if the system is terminated by  $Z_0$  ( $a_3 = a'_0 = 0$ ).

## CONTRIBUTIONS OF TWO-PORT ERROR CORRECTION USING SELF-CALIBRATION TECHNIQUE

- REDUCES THE LINEAR SYSTEM ERRORS
- REMOVES SWITCH REPEATABILITY ERRORS
- CALIBRATION STANDARDS ARE NOT CRITICAL

There are many advantages to the self-calibration technique. It is not necessary to know all the characteristics of the standards. The  $Z_0$  impedance of the air line is the only critical parameter. The frequency does not need to be extremely accurate, only repeatable. This technique is also applicable to unusual transmission media. For example, this would be an excellent calibration technique for microstrip or stripline where the section of line of an unknown length becomes the standard. Good open and short circuits are also hard to achieve in microstrip, but the self-calibration technique does not require precise terminations. Switch repeatability errors can also be removed, yielding extremely accurate and repeatable measurements.

This seminar has not discussed all of the available techniques. It has discussed only those that currently have the most impact and are most widely used.



MARCH 1982

PRINTED IN U.S.A.